Average Backscatter Clutter Power for RF Sensing Applications in Indoor Environments

Dmitry Chizhik[1], Jinfeng Du[1], Jakub Sapis[1], Reinaldo A. Valenzuela[1], Abhishek Adhikari[2], Gil Zussman[2], Manuel A. Almendra[3], Mauricio Rodriguez[3], and Rodolfo Feick[4]

[1]Nokia Bell Labs, Murray Hill, NJ 07974, USA

[2]Columbia University, New York, NY

[3]Escuela de Ingeniería Eléctrica de la Pontificia Universidad Católica de Valparaíso, Valparaíso, Chile

[4]Department of Electronics, Universidad Técnica Federico Santa Maria, Valparaíso, Chile

***Abstract*— A simple model for average backscatter power from clutter is developed for indoor RF sensing applications and verified through measurements. A narrowband 28 GHz sounder used a quasi-monostatic radar arrangement with an omnidirectional transmit antenna illuminating an indoor scene and a spinning horn receive antenna less than 1 m away collecting backscattered power as a function of azimuth. Median average backscatter power was found to vary over a 12 dB range, with average power generally decreasing with increasing room size. A deterministic model of average backscattered power dependent on distance to nearest wall and clutter reflection coefficient reproduces observations with 4.0 dB RMS error.**

Index terms— **sensing, backscatter.**

I. INTRODUCTION

There is an increasing interest [1][2][3][4] in the joint use of communication signals for sensing, often termed Joint/Integrated Communications and Sensing (JCAS or ISAC). The new functionality is essentially that of radar, aiming at detecting and possibly characterizing some aspect of the environment. Often the ambition is to detect and localize a static or moving object, termed "target", such as a person, vehicle, robot, or UAV, in the presence of the rest of the environment, the response to which is termed "clutter".

Some of the applications of indoor sensing radars being discussed [5] include detection of people, robots in indoor spaces for safety (collision avoidance in factories, frail person in room monitoring in healthcare settings), security (intruder detection). In these applications, the person/robot is either standing or lying on the floor.

Clutter echoes are often stationary, e.g., buildings outdoors, walls and furniture indoors but may also include moving objects such as people, vehicles, as well as vegetation and various street furniture that swing with the wind. Sensing scenarios of interest include monostatic, with collocated transmitter/receiver measuring backscatter, e.g., a single base station or terminal, as well as bi-static where transmitter and receiver are separated, e.g., signal traveling from one base station to another, scattering along the way. Various use cases for joint communication and sensing are under consideration by the 3GPP[18].

Algorithms for detection, localization and, possibly, classification, of objects need to be tested in realistic scenarios, requiring representative models of both clutter and target. It is desirable for the model to be easily implementable. 3GPP TR 38.901 [6]) describes communication models which have been adopted in proposals for statistical channel models for communications and sensing[8][9][10]. While such formulations are very general, determination of properties such as strength of backscatter remains open, particularly for clutter. Clutter may be viewed as either an extended object or a collection of many objects. Backscatter from clutter is then critically dependent on the number and scattering strength of such objects, as well as multiple scattering from them. This information is not available from current 3GPP communication channel models or single object target models developed in radar.

In this work we propose a measurement-based monostatic indoor backscatter model. Narrowband measurements of arriving backscatter power as a function of azimuth at 28 GHz were collected in 3 cities in 251 indoor locations in rooms of different sizes, allowing formulation of a model for indoor backscatter validated though a statistically significant data set, in environments containing both metal and dielectric materials.

Based on the data, the backscatter power ratio is represented as varying over azimuth about an average, with variation statistics derived from measurements. Azimuthal power spectra measured at locations every 10 cm allowed an assessment of variability at closely spaced locations. Key results include:

- Average measured clutter backscatter power ratio was found to generally decrease with increasing room size.
- A simple theoretical model for average backscatter as a function of distance to nearest illuminated wall was derived, with 4.0 dB RMS error.

II. Backscatter From Clutter

Received radar power of a signal scattered from an object R_o meters away with effective radar cross-section (RCS) σ_{scat} located at distance R_s meters away from the transmitter is given by the radar equation[14]:

$$P_R = \frac{\lambda^2}{4\pi}\frac{1}{4\pi R_o^2}\sigma_{scat}\frac{1}{4\pi R_s^2}P_T G_T(\Omega_{inc})G_R(\Omega_{scat}) \quad (1)$$

where λ is carrier wavelength, P_T is the transmit power, G_T and G_R are the antenna gains, and Ω_{inc} and Ω_{scat} are the angles of incidence and scattering, respectively.

For the quasi-monostatic antenna arrangement studied here, distances and angles from transmitter and receiver antennas to target are the same, with target backscatter power defined as:

$$P_{target} = \frac{\lambda^2\sigma_{back}P_T G_T G_R}{(4\pi)^3 R^4} \quad (2)$$

The above equations apply when the distance R, and antenna gains G_T, G_R do not change substantially over the extent of the target. This still allows for scattered power fluctuation due to fluctuation in σ_{back}, stemming from relative phase variation of scattered signals from different parts of the target.

In the case of an extended scatterer, such as a rough wall or a dense collection of distributed scatterers, (1) generalizes [12] to an integral over the surface of the extended scatterer:

$$P_{clut} = \frac{\lambda^2 P_T}{(4\pi)^3}\iint dA\; G_T(\Omega)G_R(\Omega)\frac{\gamma_{back}(\Omega)}{R^4} \quad (3)$$

With $\gamma_{back}(\Omega)$ a (unit-less) backscattering cross-section of the clutter surface per unit area.

A quantity of particular interest here is the backscatter power ratio for clutter:

$$P_{back} = \frac{P_{clut}}{P_T} \quad (4)$$

III. Measurement Description

The radar measurement set-up was adopted from a narrowband channel sounder [13]. The transmitter emitted a 28 GHz CW tone at 22 dBm from an omnidirectional antenna. The receiver is a 10° (24 dBi) horn, mounted on a rotating platform allowing a full angular scan every 200 ms. The receiver records power samples at a rate of 740 samples/sec. using an onboard computer. The omnidirectional transmit antenna, with vertical beamwidth of about 70°, was placed on a lower shelf of a plastic cart (Fig. 1), about 0.4 m above the floor to illuminate the surrounding area uniformly in all azimuthal directions. The spinning horn was placed on an upper shelf of the cart, about 0.7 m above the lower shelf. Multiple layers of absorbing foam, separated with aluminum foil attenuating the direct Tx-Rx signal path. This antenna arrangement was designed particularly for detecting objects close to the floor. A similar arrangement with receiver still on the upper cart shelf but the transmitter placed above the receiver, about 2 m above the floor was also used to assess the effect of transmitter height.

This monostatic radar arrangement was calibrated by measuring backscattered power from a standard trihedral target with known [16]Radar Cross-Section (RCS) in an anechoic chamber. Measured backscattered power was within 1.4 dB of prediction by (2).

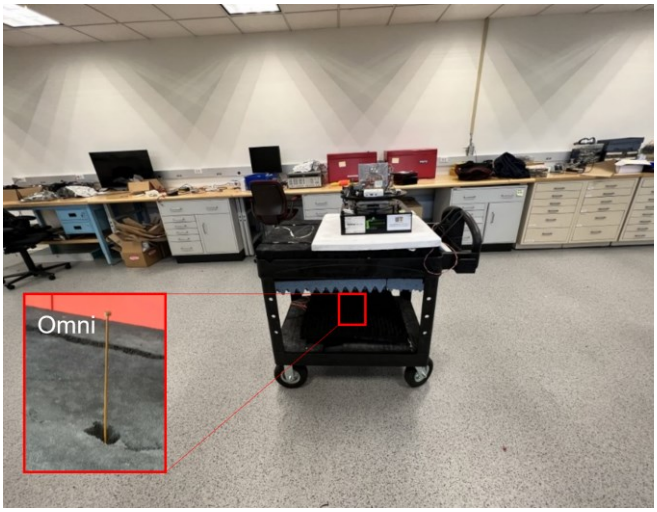

Fig. 1. 28 GHz narrowband backscatter radar arrangement, with omnidirectional Tx antenna on lower cart shelf illuminating the scene and a spinning horn receiver collecting backscatter power vs. azimuth on top cart shelf.

IV. Backscattered Power

The cart was placed in 251 locations in rooms of varying sizes, from 3x3 m offices to 20x30 m cafeteria, collecting backscatter azimuth spectra like one shown in Fig. 2. Some rooms had metal furniture and metalized windows, others wooden furniture and plain glass windows. The data was collected in 3 different building types in New York City, New Jersey office building and a university building in Chile. Room materials varied, with some rooms containing metal furniture along the walls, others with primarily wood furniture and drywall walls. We measured 81, 128 and 42 small, medium, and large office locations, with distances to nearest illuminated wall of under 2.5, 3-5 m, and greater than 5 m, respectively. A general observation was that backscattered power ratio in any direction may be characterized statistically by variation around an average value over azimuth:

$$\langle P_{back}\rangle_\phi = \frac{\langle P_{clut}\rangle_\phi}{P_T} \quad (5)$$

indicated as a dashed circle in Fig. 2. The observed average backscatter value varied from location to location, with cumulative distributions, grouped by room size, plotted in Fig. 3. For display clarity, Fig. 3 shows a representative set of 73 links collected in rooms with metal furniture and /or metalized windows. It is observed that average backscatter power

generally decreases as the room size increases. Similar conclusions were reached for data collected using a transmitter above the receiver, about 2m above the floor.

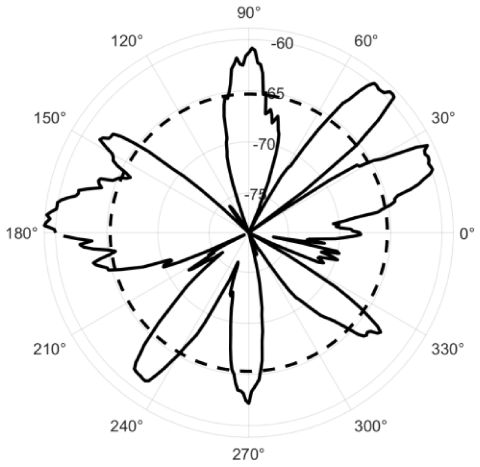

Fig. 2 Sample measured backscattered power ratio vs. azimuth. Dashed line is average backscattered power ratio (5)

In these measurements, the radar transceiver is placed near the center of a room, with the visually observed clutter consisting of furniture and other objects, such as lab instruments, near walls, with clutter at distance d_s that generally varies with direction. Viewing such clutter as an extended scatterer at distance d_s from the transceiver, as illustrated in Fig. 4, we evaluate the corresponding theoretical backscatter ratio (3) for comparison against measurements. Since the illuminated area at any one antenna orientation included many objects, often of irregular shape, it is not meaningful to assign an incidence angle on the surface. The scattering is then characterized generically as a scattering coefficient γ_{back}. To account for material properties, the scattering coefficient is set to Fresnel reflection coefficient, averaged over a uniform distribution of incidence angles, representing incidence on (unresolved) object facets:

$$\gamma_{\text{back}}(\Omega) = \left\langle \left|\Gamma_{\text{clut}}\right|^2 \right\rangle \tag{6}$$

Where $\left|\Gamma_{\text{clut}}\right|^2$ is the material-dependent reflection coefficient.

The scattered power integral (3) may be evaluated, particularly simply in the case of interest here, where the integrand behavior is defined by the beamspot cast on the clutter region by the directive receive antenna (10° beamwidth in these measurements):

$$G_{\text{R}}(\phi,\theta) = \frac{2}{\phi_{\text{RMS}}\theta_{\text{RMS}}} e^{-\phi^2/2\phi_{\text{RMS}}^2} e^{-\theta^2/2\theta_{\text{RMS}}^2} \tag{7}$$

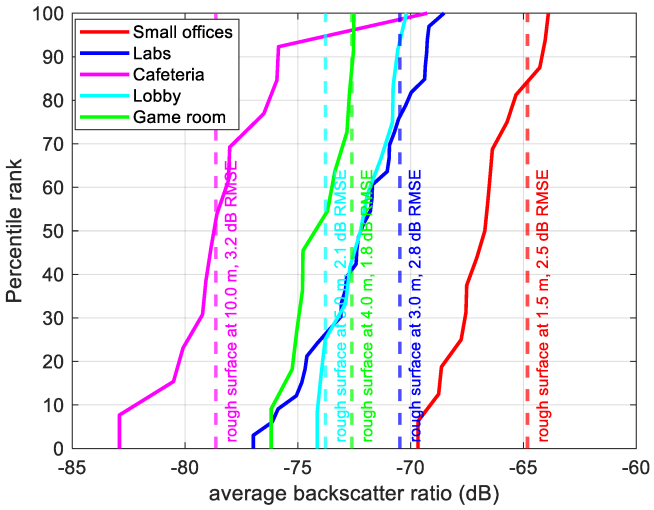

Fig. 3. Distributions of measured locally averaged backscatter power ratios (5) in rooms of different sizes. Dashed vertical lines are predictions by (9), with distance to wall as indicated

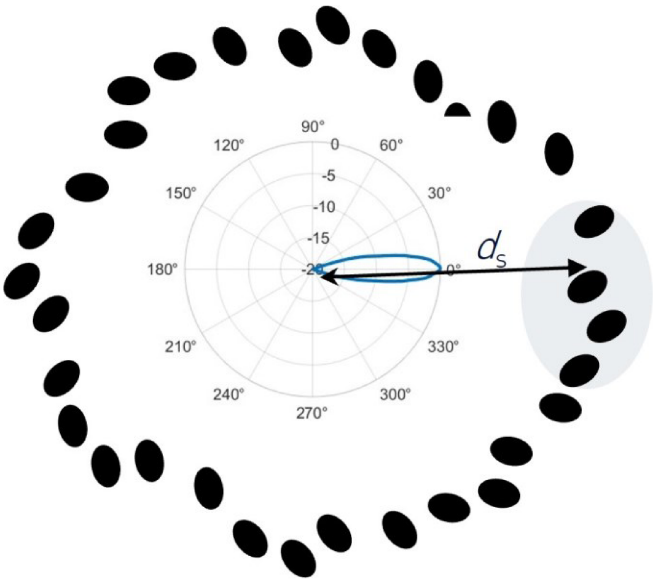

Fig. 4. Backscatter geometry for calculation of average backscatter

$$\begin{aligned}\left\langle P_{\text{clut}} \right\rangle_{\phi} &= \frac{\lambda^2 P_{\text{T}} \left\langle \left|\Gamma_{\text{clut}}\right|^2 \right\rangle}{(4\pi)^3} \iint dA \;\; G_{\text{R}}(\phi,\theta) G_{\text{T}}(\phi,\theta) \frac{1}{R^4} \\ &= \frac{\lambda^2 P_{\text{T}} \left\langle \left|\Gamma_{\text{clut}}\right|^2 \right\rangle 2G_{\text{T}} d_s^2}{(4\pi)^3 \phi_{\text{RMS}}\theta_{\text{RMS}} d_s^4} \int_{-\pi/2}^{\pi/2} d\theta \; e^{-\theta^2/2\theta_{\text{RMS}}^2} \int_{-\pi}^{\pi} d\phi e^{-\phi^2/2\phi_{\text{RMS}}^2} \\ &\approx P_{\text{T}} G_{\text{T}} \left\langle \left|\Gamma_{\text{clut}}\right|^2 \right\rangle \left(\frac{\lambda}{4\pi d_s}\right)^2 \end{aligned} \tag{8}$$

Where differential area $dA = d_s^2 d\theta d\phi$, and $R \approx d_s$. The transmit antenna is assumed to have a much broader beamwidth than the receive antenna, aimed in the same direction. In measurements done here an omni antenna was used in the

transmitter, with G_T=1. In evaluating (8) it was assumed that the integrand effective angular support is defined primarily by the directivity of the (receive) antenna, as appropriate for the 10° antenna used in measurements in this work. Under these conditions the average backscattered power P_{clut} is independent of the antenna patterns.

Average backscattered power ratio can thus be defined in terms of environment quantities alone:

$$\langle P_{back} \rangle = \frac{\langle P_{clut} \rangle_{\phi}}{P_T} = \left\langle \left| \Gamma_{clut} \right|^2 \right\rangle \left(\frac{\lambda}{4\pi d_s} \right)^2 \quad (9)$$

Average backscatter ratio predicted by (9) is evaluated for different room sizes and compared against measurements in Fig. 3. Rooms with steel furniture dominating the field of view of antennas (as in Fig. 1), and metalized windows, were assigned $\left\langle \left| \Gamma_{clut} \right|^2 \right\rangle = 1$ in (9), while rooms with wooden furniture were assigned $\left\langle \left| \Gamma_{clut} \right|^2 \right\rangle = 0.25$, corresponding to the power reflection coefficient from air-dielectric interface with relative dielectric constant of 3 [17](representative of dry wall/wood), averaged over a uniform distribution of incidence angles over 0-90°. Distance to clutter d_s was set to distance to nearest wall used in measurements, typically d_s=half the smallest dimension of the room. Formula (9) prediction is indicated as corresponding vertical lines in Fig. 3 for various room sizes. Overall RMSE error is found to predict measured average backscatter ratio with 4.0 dB RMS error, notable considering the medians of the observed distributions span some 12 dB. The sole parameters in (9) are the distance d_s to nearest illuminated wall and material-dependent reflection coefficient $\left\langle \left| \Gamma_{clut} \right|^2 \right\rangle$ of 1 or 0.25, for metal/dielectric surroundings, respectively.

V. Conclusions

A simple statistical monostatic radar channel model for average power backscattered from clutter is developed for indoor applications, requiring only room dimensions and a representative dielectric constant. A narrowband 28 GHz sounder was used in a quasi-monostatic antenna arrangement with an omnidirectional transmit antenna illuminating the scene and a spinning horn receive antenna collecting backscattered power as a function of azimuth. Average backscatter power ratio was found to vary over a 12 dB range, with average power generally decreasing with increasing room size. A deterministic model of average backscattered power dependent only on average distance to clutter reproduces observations with 4.0 dB RMS error.

Acknowledgements

Thanks to David Chen (Stuyvesant High School) and Timothy Wang (University of Michigan) for assistance in measurements. A. Adhikari and G. Zussman wish to acknowledge the support through NSF grants EEC- 2133516, CNS-2148128, AST-2232. M. A. Almendra, M. Rodriguez, and R. Feick wish to acknowledge the support received from the Chilean Research Agency ANID, through research grants ANID FONDECYT 1211368, and ANID PIA/APOYO AFB220004; and the project VRIEA-PUCV 039.367/2023.

References

[1] R. Cager, D. LaFlame and L. Parode, "Orbiter ku-band integrated radar and communications subsystem", IEEE Transactions on Communications, vol. 26, no. 11, pp. 1604-1619, Nov. 1978.

[2] C. W. Rossler, E. Ertin and R. L. Moses, "A software defined radar system for joint communication and sensing," 2011 IEEE RadarCon (RADAR), Kansas City, MO, USA, 2011.

[3] M. Alloulah and H. Huang, "Future Millimeter-Wave Indoor Systems: A Blueprint for Joint Communication and Sensing," in Computer, vol. 52, no. 7, pp. 16-24, July 2019.

[4] T. Wild, V. Braun and H. Viswanathan, "Joint Design of Communication and Sensing for Beyond 5G and 6G Systems," in IEEE Access, vol. 9, pp. 30845-30857, 2021.

[5] Study on Integrated Sensing and Communication, 3GPP TR 22.837, June, 2023.

[6] *Technical Specification Group Radio Access Network; Study on Channel Model for Frequencies From 0.5 to 100 GHz* (Release 17), 3GPP TR 38.901 v.17.0.0, March 2022.

[7] E. M. Vitucci, V. Degli-Esposti, F. Fuschini, J. S. Lu, M. Barbiroli, J. N. Wu, M. Zoli, J. J. Zhu, H. L. Bertoni, "Ray Tracing RF Field Prediction: An Unforgiving Validation", International Journal of Antennas and Propagation, vol. 2015.

[8] R. Yang, C. -X. Wang, J. Huang, E. -H. M. Aggoune and Y. Hao, "A Novel 6G ISAC Channel Model Combining Forward and Backward Scattering," in IEEE Transactions on Wireless Communications, doi: 10.1109/TWC.2023.

[9] Z. Zhang et al., "A General Channel Model for Integrated Sensing and Communication Scenarios," in IEEE Communications Magazine, vol. 61, no. 5, pp. 68-74, May 2023

[10] A. Bhardwaj, D. Caudill, C. Gentile, J. Chuang, J. Senic and D. G. Michelson, "Geometrical-Empirical Channel Propagation Model for Human Presence at 60 GHz," in IEEE Access, vol. 9, pp. 38467-38478, 2021.

[11] D. Chizhik, J. Du, M. Kohli, A. Adhikari, R. Feick; R. A. Valenzuela, "Accurate Urban Path Loss Models Including Diffuse Scatter", 17th European Conf. on Antennas and Prop. (EuCAP), Florence, Italy, 2023.

[12] G. T. Ruck, D. E. Barrick, W. D. Stuart, C. K. Krichbaum, *Radar Cross Section Handbook*. Vol. 1 & 2, Plenum Press, Jan. 1, 1970.

[13] D. Chizhik, J. Du, R. Feick, M. Rodriguez, G. Castro, and R. A. Valenzuela, "Path loss and directional gain measurements at 28 GHz for non-line-of-sight coverage of indoors with corridors", *IEEE Trans. Antennas Propag.*, vol. 68 (6), pp. 4820–4830, Jun. 2020.

[14] M. Skolnik, Introduction to Radar Systems: Third Edition. McGraw-Hill, New York, 2001.

[15] *IEEE 802.11 Wireless LANs Channel Models for WLAN Sensing Systems*, IEEE 802.11-21/0782r5, August 2021.

[16] https://www.eravant.com/2-4-edge-length-trihedral-corner-reflector.

[17] S. S. Zhekov, O. Franek and G. F. Pedersen, "Dielectric Properties of Common Building Materials for Ultrawideband Propagation Studies", *IEEE Antennas and Propagation Magazine*, Feb. 2020.

[18] "Feasibility Study on Integrated Sensing and Communication (Release 19)", 3GPP TR 22.837 V19.1.0 (2023-09), Technical Report, 3rd Generation Partnership Project; Technical Specification Group TSG SA.